PLASTID GENOMES OF THE HEMIPARASITIC GENUS *KRAMERIA* (ZYGOPHYLLALES) ARE INTACT AND EXHIBIT LITTLE RELAXATION IN SELECTION

Arjan Banerjee,[1,*,†] Adam C. Schneider,[2,*,‡] and Saša Stefanović*

*Department of Biology, University of Toronto Mississauga, Mississauga, Ontario L5L 1C6, Canada; †Ecology and Evolutionary Biology, University of Toronto, Toronto, Ontario M5S 2Z9, Canada; and ‡Department of Biology and Health Sciences, Hendrix College, Conway, Arkansas 72032, USA

Editor: Susan J. Mazer

Premise of research. Parasitic plants are characterized by a reduced or absent ability to conduct photosynthesis and accompanying morphological, physiological, and genomic changes. The plastid genome (or plastome) houses many key photosynthetic genes and is consequently highly conserved in autotrophic plants. This molecule is thus a useful model for documenting the genomic effects of a loss of autotrophy, which is typically associated with some reduction in plastome size and coding content. Twelve lineages of angiosperms have seen independently evolved haustorial parasitism. One of these lineages, *Krameria*, is a genus of obligate hemiparasites that appears to subvert the expectation of plastome reduction and instead has a substantially longer plastid genome than its nearest photosynthetic relatives.

Methodology. Two plastid genomes have been reported from this genus but have not yet been analyzed in depth. This study adds a third assembled *Krameria* plastome and then investigates their structure and sequence composition in comparison with that of the autotrophic *Tribulus terrestris* from the group's sister clade.

Pivotal results. We find that *Krameria* plastomes have essentially intact coding sequences and that the unexpected increase in their sizes is due to the accumulation of elevated numbers of tandem repeats in the intergenic spaces of the large and small single-copy regions. Photosynthetic genes are maintained under purifying selection with *dN*/*dS* values commensurate with those observed in lineages of autotrophic plants.

Conclusions. *Krameria* contains both the largest and the most intact plastid genomes reported to date from parasitic angiosperms. Our results suggest that these plants are still reliant on photosynthesis as an important part of their nutrient acquisition strategy and that plastid genomes of *Krameria* remain evolutionarily stable.

Keywords: hemiparasites, heterotrophs, *Krameria*, Krameriaceae, parasite, plastid, plastome.

Online enhancements: supplemental tables.

Introduction

One of the most remarkable examples of convergent evolution is the repeated origin of heterotrophy in plants accompanied by a suite of morphological, genomic, ecological, and life history shifts, often referred to as the "parasite reduction syndrome" (Colwell 1994). Plants achieve heterotrophy by one of two modes: parasitizing mycorrhizal fungi (mycoheterotrophy) or forming direct vascular connections with the roots or stems of other spermatophytes using a specialized organ called a haustorium. Both modes have evolved many times—there have been more than 40 origins of mycoheterotrophy (Merckx 2013; Jacquemyn and Merckx 2019) and 12 origins of direct parasitism (Nickrent 2020; fig. 1)—in aggregate providing the statistical power to develop and test more generalized models for the evolution of parasitic plants.

Among these models of evolution, recent interest (Shin and Lee 2018; Su et al. 2019; Banerjee and Stefanović 2020) has focused on the parasitic plant plastid genome (plastome), which contains many genes involved in key portions of the photosynthetic apparatus in addition to so-called housekeeping genes responsible for the ongoing functionality of the plastome itself (Wicke et al. 2011). A model developed by Wicke et al. (2016) predicts relaxation of purifying selection followed by gene pseudogenization and loss in five distinct consecutive categories of plastid genes that are increasingly central to plastome function

[1] Author for correspondence; email: arjan.banerjee@mail.utoronto.ca.
[2] Current address: Department of Biology, University of Wisconsin–La Crosse, 1725 State Street, La Crosse, Wisconsin 54601, USA

Manuscript received December 2021; revised manuscript received March 2022; electronically published April 28, 2022.

  Published by The University of Chicago Press. https://doi.org/10.1086/719959

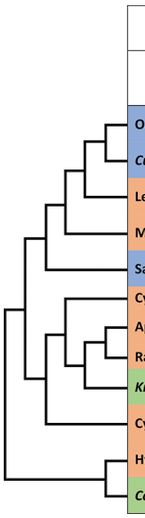

				Largest Plastome				Smallest Plastome			
Lineage	Parasitic Status	Number of Species‡	Plastome Size Range (kb)	Species	Size (bp)	Gene Composition (protein/tRNA/rRNA)	Ref	Species	Size (bp)	Gene Composition (protein/tRNA/rRNA)	Ref
Orobanchaceae	Mix	2100	46-161	*Conopholis americana*	45,673	21/18/4	a	*Schwalbea americana*	160,911	74/30/4	a
Cuscuta	Mix	200	61-125	*Cuscuta erosa*	60,959	33/25/4	b	*Cuscuta exaltata*	125,373	67/29/4	c
Lennoaceae	Hol	4	81-84	*Pholisma arenarium*	81,198	27/29/4	d	*Lennoa madreporioides*	83,675	27/29/4	d
Mitrastemonaceae	Hol	2	26	*Mitrastemon kanehirai**	25,740*	17/4/2	e				
Santalales	Mix	2357	17-158	*Balanophora laxiflora**	15,505*	15/1/4	f	*Malania oleifera*	158,163	62/30/4	g
Cytinaceae	Hol	12	19	*Cytinus hypocistis*	19,400	14/6/4	h				
Apodanthaceae	Hol	10	11-15	*Pilostyles aethiopica*	11,348	3/0/2	i	*Pilostyles hamiltonii*	15,167	4/0/2	i
Rafflesiaceae	Hol	30	—△		—△						
Krameria	Hem	23	172-173	*Krameria lanceolata*	171,851	78/30/4	j	*Krameria bicolor*	172,606	78/30/4	j
Cynomoriaceae	Hol	2	46	*Cynomorium coccineum*	45,519	18/4/4	k				
Hydnoraceae	Hol	12	27-28	*Hydnora visseri*	27,233	17/4/4	l	*Prosopanche americana**	28,191*	15/5/4	m
Cassytha	Hem	20	115	*Cassytha filiformis*	114,622	67/30/4	n	*Cassytha capillaris*	115,151	67/30/4	o

Fig. 1 Summary of the 12 angiosperm lineages that have seen the independent evolution of parasitism. The smallest reported plastid genomes are described for each lineage except for *Rafflesiaceae*, where the plastid genome is deemed absent. The largest known plastid genomes are also described for lineages for which multiple plastomes have been published. References for each plastome are listed. Holoparasitic lineages are highlighted in orange, hemiparasitic lineages in green, and mixed lineages in blue. Phylogenetic relationships between the different lineages are shown on the left and are taken from Angiosperm Phylogeny Group IV (Catalogue of Life Partnership 2017). A plus/minus sign indicates that estimates of the number of species are based on Nickrent (2020). An asterisk indicates that plastomes for *Mitrastemon kanehirai* (MF372930), *Balanophora laxiflora* (KX784265), and *Prosopanche americana* (MT075717) have been submitted to GenBank but have not been verified by National Center of Biotechnology Information staff. A triangle indicates that research on *Rafflesia lagascae* (Molina et al. 2014) and *Sapria himalayana* (Cai et al. 2021) shows that the plastid genome may be lost in Rafflesiaceae. hem = hemiparasitic; hol = holoparasitic; mix = mixed lineages. References: a = Wicke et al. (2013); b = Banerjee and Stefanović (2019); c = McNeal et al. (2007); d = Schneider et al. (2018); e = S. Y. Shyu and J. M. Hu (unpublished work); f = Chen et al. (2020); g = Yang and He (2019); h = Roquet et al. (2016); i = Bellot and Renner (2015); j = Gonçalves et al. (2019); k = Bellot et al. (2016); l = Naumann et al. (2016); m = Jost et al. (2020); n = Wu et al. (2017); o = Liu et al. (2021).

(Barrett and Davis 2012; Barrett et al. 2014; Wicke and Naumann 2018). Indeed, among the many lineages of parasitic plants studied, most show this relaxation of purifying selection and reductions in sequence length and gene content, even though those of their closely related autotrophs are highly conserved (Graham et al. 2017; Wicke and Naumann 2018).

Aside from those of two species of endoparasitic Rafflesiaceae that are thought to have lost their plastomes entirely (Molina et al. 2014; Cai et al. 2021), plastomes from all lineages of haustorial parasites have now been sequenced (fig. 1). As predicted by the abovementioned models of plastome evolution in such plants (Wicke et al. 2016; Graham et al. 2017), most of these lineages exhibit some degree of reduction relative to their nearest autotrophic relatives in terms of both size and sequence composition (fig. 1). The variability in these reductions can generally be explained by the position of the respective lineages on the trophic continuum: holoparasitic plants are expected to have more reduced plastomes than hemiparasitic plants because of their diminished (or absent) reliance on the photosynthetic genes that plastomes primarily encode. Among hemiparasitic plants, obligate hemiparasites may be expected to show more conspicuous plastome reduction than facultative hemiparasites, which use parasitism as a supplementary means of nutrient acquisition rather than as a principal strategy.

One lineage noticeably subverts this expectation (fig. 1). The genus *Krameria* is a group of ca. 23 species of obligate root hemiparasites found throughout hot, dry, or seasonally dry environments in North and South America (Simpson 1989; Nickrent 2020). Like several other parasitic lineages (Heide-Jorgensen 2008), *Krameria* species appear to establish only xylem connections with their hosts (Brokamp et al. 2012). The phylogenetic position of this genus has historically been the matter of some debate. Cronquist (1981) placed it as part of a monogeneric family, Krameriaceae, in Polygalales (Rosidae). Recent phylogenetic analyses based on nuclear and plastid data have confirmed the monotypic nature of Krameriaceae but place it sister to the family Zygophyllaceae, together comprising order Zygophyllales, positioned as sister to the rest of the fabids (Sheahan and Chase 1996; Soltis et al. 2000; Wang et al. 2009; Angiosperm Phylogeny Group et al. 2016). Despite the fact that *Krameria* individuals cannot survive without their hosts (Simpson 1989), the two reported plastomes from this genus, in the species *K. bicolor* S. Watson (synonym, *K. grayi* Rose and J.H. Painter) and *K. lanceolata* Torr., are substantially longer (ca. 172–173 kb) than those of their nearest autotrophic relatives, *Tribulus terrestris* L. (ca. 158 kb; Yan et al. 2019) and *Larrea tridentata* (DC.) Coville (ca. 136 kb; Gonçalves et al. 2019), and appear to show no reduction in gene composition. Although these plastid genomes were used for phylogenetic purposes, they have not yet been characterized in depth in terms of structural makeup and sequence divergence, and several key questions remain unanswered. Namely, are photosynthesis-related protein-coding genes in *Krameria* under reduced purifying selection compared with those of autotrophs? Why are the sizes of *Krameria* plastomes larger when we would expect sequence length reduction? Are coding regions affected? If so, is the increase in sequence size simply an unusual manifestation

of the parasitic syndrome, with an incidental increase in genome size instead of a reduction? To answer these questions, we compared the gene content and selection of plastomes of three *Krameria* species (one newly sequenced) with those of closely related autotrophs in the Zygophyllaceae.

Methods

Taxon Sampling, DNA Extraction, and Sequencing

Total genomic DNA was isolated from silica-dried tissue of *Krameria erecta* Willd. (collection: Stefanović SS-16-22, deposited in the TRTE herbarium) using the modified cetyltrimethylammonium bromide method (Doyle and Doyle 1987) and was checked for quantity and quality using a NanoDrop 1000 Spectrophotometer (Thermo Fisher Scientific). This extraction was sequenced on an Illumina HiSeq 2500 platform (2 × 126-bp paired-end reads; Centre for Applied Genomics, SickKids Hospital, Toronto, ON). Demultiplexing of raw reads and the removal of indexing barcodes were performed by the sequencing facility.

Plastome Assembly, Annotation, and Computational Methods

Krameria erecta reads were trimmed using Sickle version 1.33 (Joshi and Fass 2011) with minimum read lengths set at 99 bp and the threshold for quality set at a minimum Phred score of 27 at each site. A total of 52,328,346 reads were recovered after the trim. Several separate assemblies were conducted de novo using distinct subsamples of reads in both Geneious R10 (Biomatters, Auckland, New Zealand; produce scaffolds and don't merge variants boxes unchecked) and GetOrganelle version 1.7.5 (Jin et al. 2020; -R set to 15, -w to 110, -k to 65, 115 and *Tribulus terrestris* plastome used as the seed file). Initial annotation was conducted in Geneious R10 and then refined and confirmed manually using BLASTn (Altschul et al. 1990), BLASTx (Altschul et al. 1990), and tRNAscan-SE 2.0 (Lowe and Chan 2016) to confirm rRNA gene sequences, establish open reading frames, and determine the boundaries of tRNA genes. Trimmed reads were mapped back to whole plastomes assembled to confirm the boundaries of annotated regions.

The annotated plastome of *K. erecta* was aligned with those of three other close relatives obtained from GenBank (*K. lanceolata*, *K. bicolor*, and *T. terrestris*; accessions MK726016, MK726015, and MN164624, respectively) using progressiveMauve (Darling et al. 2010) to identify any structural differences. The Phobos version 3.3.12 tandem repeat search tool (http://www.rub.de/ecoevo/cm/cm_phobos.htm) was used to identify tandem repeats, with 2–7-bp motifs defined as short tandem repeats and 8–20-bp motifs defined as medium-length tandem repeats. Selection analyses were conducted for all 78 protein-coding genes in the plastome. Gene sequences extracted from each of the three *Krameria* species were aligned pairwise with the corresponding genes of *T. terrestris* using MUSCLE (Madeira et al. 2019) in the multiple sequence alignment package version 1.18 (Bodenhofer et al. 2015) of R version 3.6.3 (R Core Team 2000). The ratio of substitution rates (*dN*/*dS*) for each gene was generated using the analysis of phylogenetic evolution package version 5.3 (Paradis et al. 2004; Popescu et al. 2012).

Results

A 177,797-bp-long closed plastid genome was assembled for *Krameria erecta* in a single contig using GetOrganelle version 1.7.5 (table 1). An identical plastome was generated in three separate contigs using the Geneious R10 native de novo assembler, and gaps were manually closed using bridging contigs from additional assemblies. Since plastomes using both methods were consistent with each another in all respects, the version produced by GetOrganelle is used hereafter and was submitted to GenBank (accession no. OL889926).

The assembled plastome of *K. erecta* is ca. 6 kb longer than the shortest *Krameria* plastome of *K. lanceolata* (table 1) and ca. 20 kb longer than the *Tribulus terrestris* plastome. However, the total coding region sizes of all four plastid genomes are within ca. 400 bp of each other (between 90.3 and 90.7 kb; table 1). All three *Krameria* plastomes maintain the standard quadripartite structure, with the size and composition of the inverted repeat regions remaining consistent (table 1). There are no structural differences or changes in synteny among the three species (fig. 2) or in comparison with *T. terrestris*. Each of the three *Krameria* plastomes retain the full complement of protein-coding and rRNA genes (table 1). *Krameria lanceolata* and *K. bicolor* also retain all plastome tRNA genes. The *trnK*-UUU is present only in a fragmented, presumably nonfunctional form in *K. erecta*, although the gene *matK*, which encodes the intron maturase and is usually present in the *trnK*-UUU intron, remains.

All plastid gene families with a bioenergetic function exhibit low values for the ratio of substitution rates (*dN*/*dS* or ω, calculated as the ratio of nonsynonymous substitutions per nonsynonymous site to synonymous substitutions per synonymous site for a given sequence) in all three *Krameria* species, except for *cemA*, which shows a moderate ω value of 0.52 (fig. 3). The average value of ω among the three plastomes is 0.23 for

Table 1

Plastid Genome Size and Structure Information for the Three *Krameria* Species Discussed in This Article and *Tribulus terrestris*

Species	GenBank accession	Plastome size (bp)	Genes (protein/tRNA/rRNA)	GC (%)	IR (bp)	IR (bp %)	Total coding regions (bp)	Coding regions (% of total)
K. bicolor	MK726015	172,606	78/30/4	33.6	26,947	15.61	90,627	53
K. lanceolata	MK726016	171,851	78/30/4	33.7	26,852	15.63	90,690	53
K. erecta[a]	OL889926	177,797	78/29/4	32.3	26,919	15.14	90,261	51
T. terrestris	MN164624	158,184	78/30/4	35.8	25,842	16.37	90,627	57

Note. IR = inverted repeat.

[a] Newly assembled.

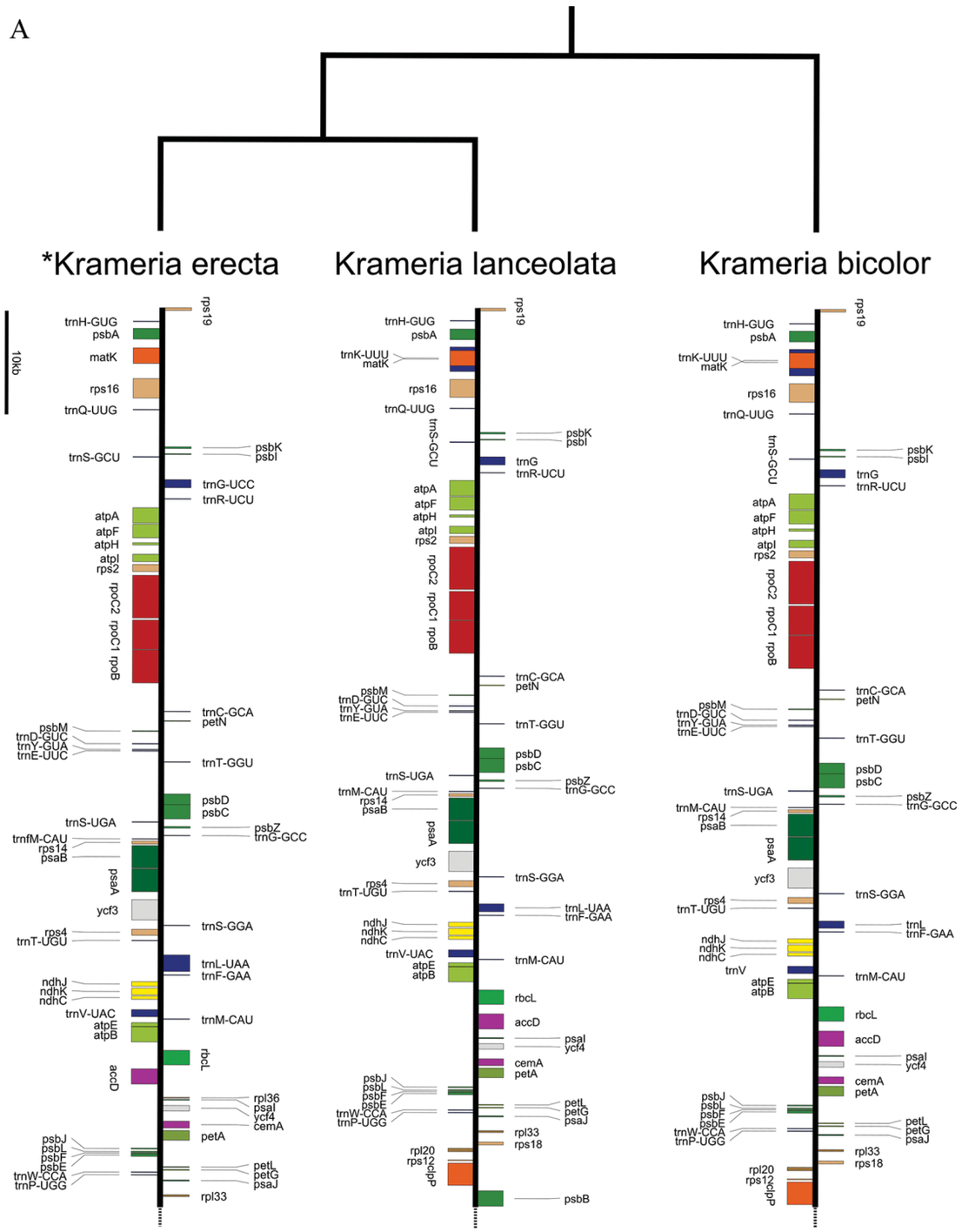

Fig. 2 Annotated plastid genomes from the three *Krameria* species. The plastome for *K. erecta* was assembled as part of this project (indicated by an asterisk), and those for *K. lanceolata* (MK726016) and *K. bicolor* (MK726015) were taken from GenBank. Labeling errors from the previously published plastomes have been corrected for *trnK*-UUU (which was mislabeled FNM##_pg002) and *trnI*-CAU (which was mislabeled *trnM*-CAU). This figure was created using OGDRAW (Greiner et al. 2019), and the cladogram follows Simpson et al. (2004).

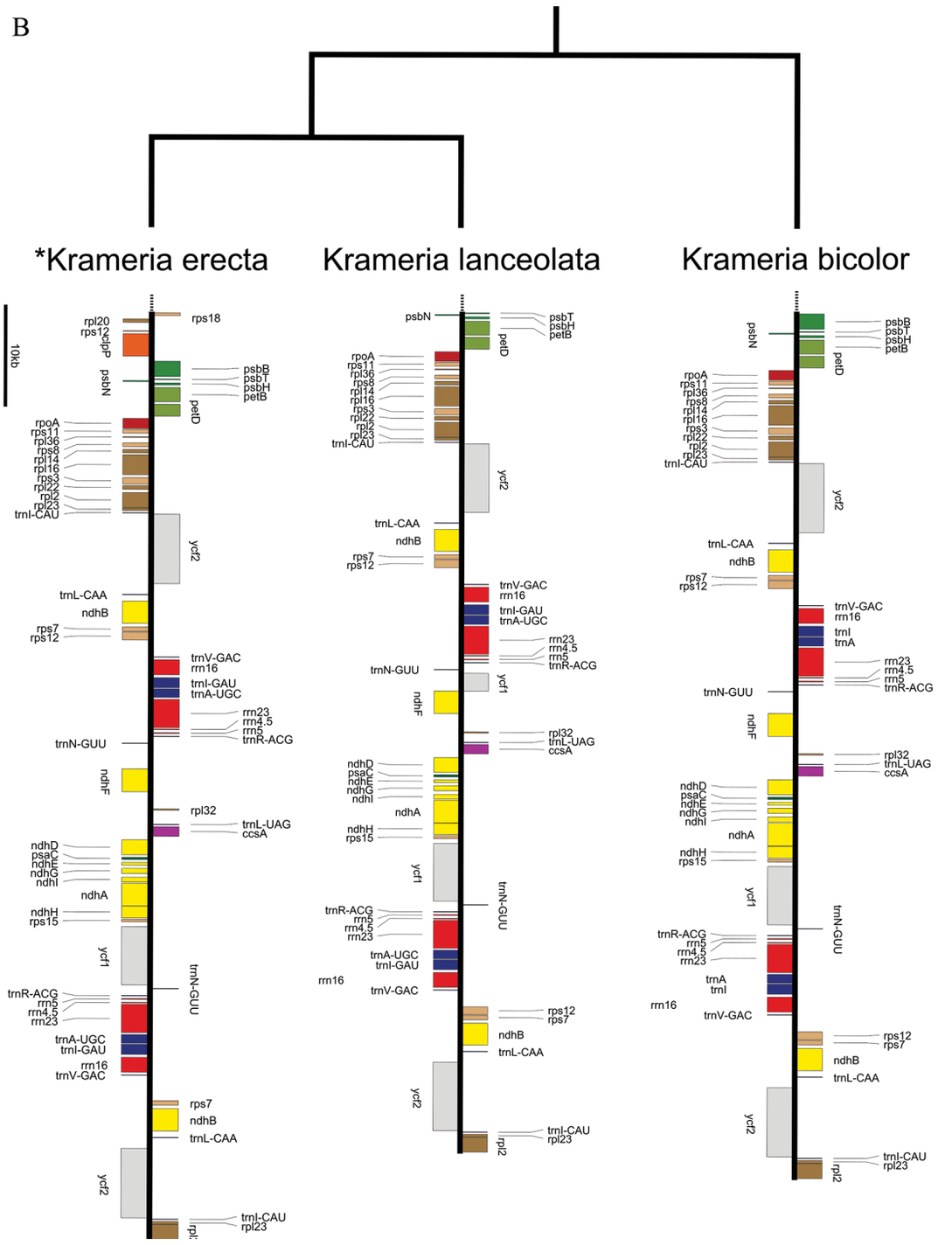

Fig. 2 (*Continued*)

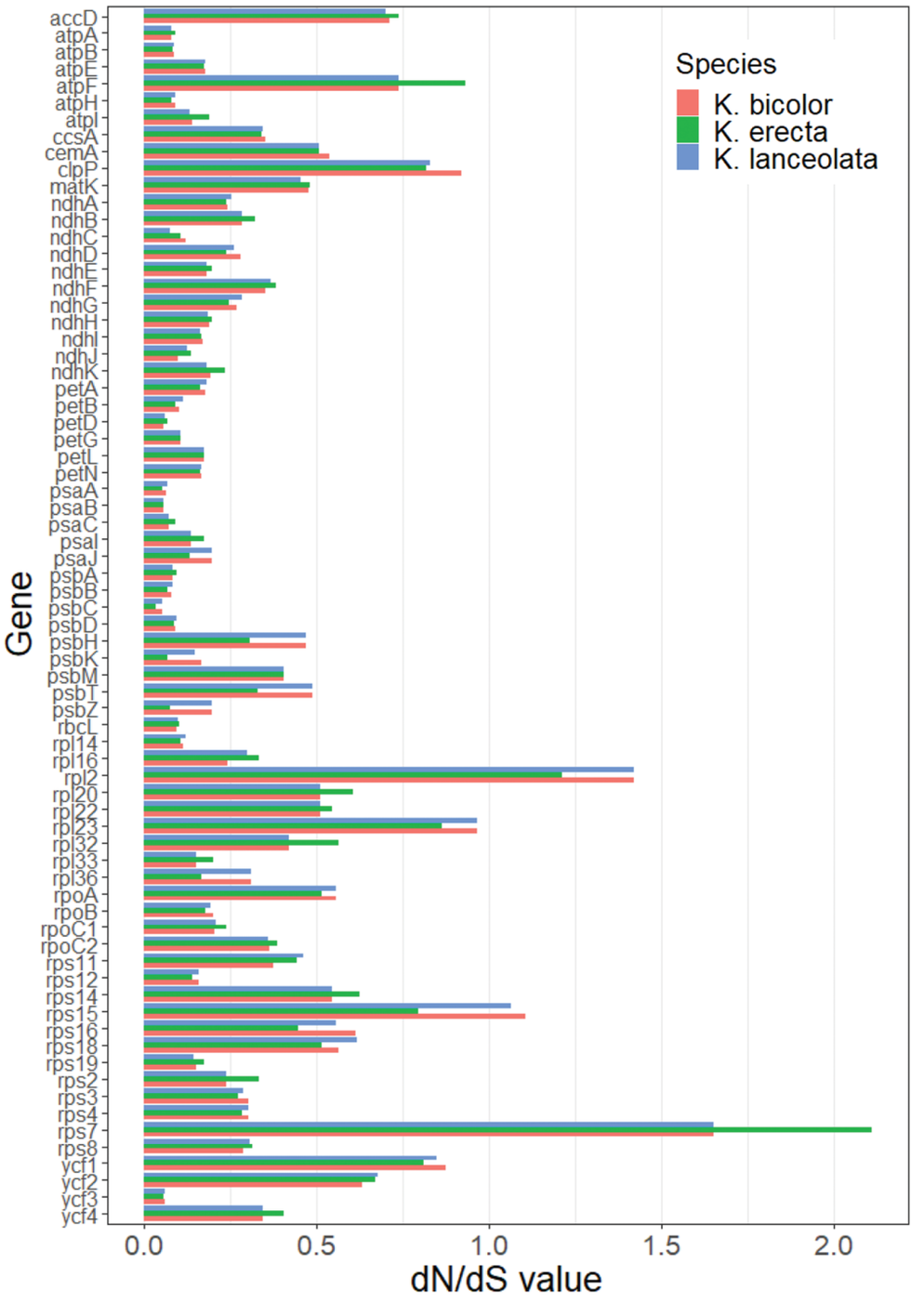

Fig. 3 Bar charts showing the substitution ratio (*dN/dS*) values for all genes present in Krameria bicolor (red), *K. erecta* (green), and *K. lanceolata* (blue). The outgroup used for the pairwise analyses was the photosynthetic *Tribulus terrestris*. Values below 1.0 indicate that the genes are under purifying selection, values greater than 1.0 indicate that the genes are under positive/diversifying selection, and values of approximately 1.0 indicate that selection is neutral. The following genes have been omitted because their *dN/dS* values equal 0: *psbE, psbF, psbI, psbJ, psbL*, and *psbN*.

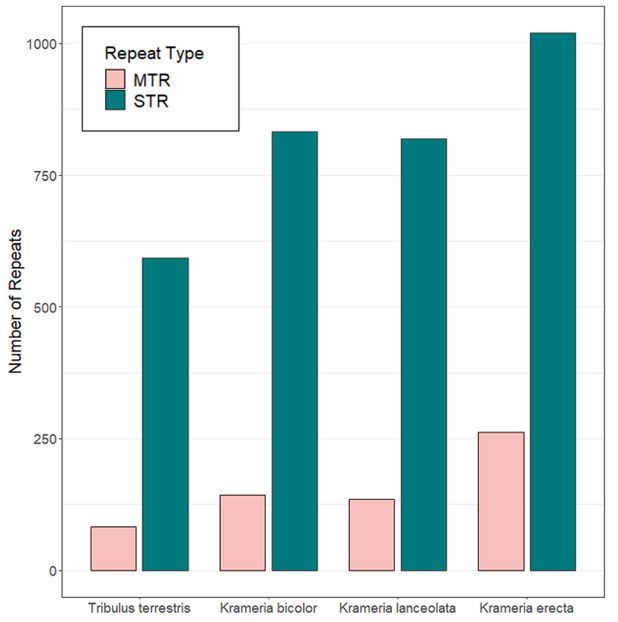

Fig. 4 Comparison of short tandem repeats (STRs; 2–7 bp; blue bar) and medium-length tandem repeats (MTRs; 8–20 bp; pink bar) in three *Krameria* species and *Tribulus terrestris*.

atp, 0.13 for *pet*, 0.10 for *psa*, 0.12 for *psb*, 0.22 for *ndh*, 0.10 for *rbcL*, 0.35 for *ccsA*, 0.06 for *ycf3*, and 0.37 for *ycf4*. Meanwhile, the four families of housekeeping genes present low to moderate ω values: 0.33 on average for *rpo*, 0.52 for *rpl*, 0.53 for *rps*, and 0.47 for *matK*. The four plastome protein-coding genes with nonbioenergetic functions exhibit higher ω values: 0.72 for *accD*, 0.86 for *clpP*, 0.85 for *ycf1*, and 0.66 for *ycf2*. A small number of ribosomal protein genes exhibit unusually elevated ω values: rpl2, rpl23, rps7, and rps15.

Krameria plastomes have elevated numbers of tandem repeat sequences compared with those of *T. terrestris*. The plastid genome of *T. terrestris* contains 593 short tandem repeats (2–7 bp) and 82 medium-length tandem repeats (8–20 bp) that in total contribute 8,766 bp of sequence length (fig. 4; detailed summary in table S1). *Krameria lanceolata* and *K. bicolor* have accumulated 819 and 832 short tandem repeats and 135 and 143 medium-length tandem repeats, respectively (fig. 4). This contributes in total 12,948 and 14,404 bp to their respective plastomes. *Krameria erecta* contains the greatest number of tandem repeats: 1020 short and 262 of medium length, in total contributing 20,169 bp (fig. 4; table S1). Tandem repeats detected in the three *Krameria* species are concentrated in the noncoding spaces of the two single-copy regions and are almost absent from the inverted repeat regions (table S1).

Discussion

Both *Krameria* plastomes previously reported (Gonçalves et al. 2019) and the *K. erecta* plastome assembled in this study retain all the plastid genes present in their autotrophic relative *Tribulus terrestris*, with the exception of *trnK*-UUU in *K. erecta* (fig. 2). The second exon of the gene is present in a divergent form, but the first exon cannot be identified, so it is presumed that *trnK*-UUU is nonfunctional. The *trnK*-UUU is often missing in parasitic plastomes (Graham et al. 2017; Li et al. 2017; Banerjee and Stefanović 2019, 2020) and almost always leaves behind a functional copy of *matK* (Hausner et al. 2006; Graham et al. 2017), which is usually encoded by its intron (i.e., *matK* is usually present within the *trnK*-UUU intron). This is the case for *K. erecta* as well. Outside parasitic lineages, *trnK*-UUU is generally conserved across seed plants, although it is absent in chlorophyte algae, monilophyte ferns (Kwon et al. 2020), and certain lycophytes (Pereira et al. 2021). This is the only instance of the gene content of *Krameria* plastomes diverging from that of their autotrophic neighbors. Such holistic retention of plastome genes is unprecedented among parasitic angiosperms (fig. 1). Previously, the most intact plastome reported was the ca. 161-kb molecule from the obligate hemiparasite *Schwalbea americana* (Wicke et al. 2013), which has five genes pseudogenized, including four *ndh* genes with a photosynthetic function.

It has been observed that the intensity of selection, in both positive and purifying directions, tends to be elevated in heterotrophic plastomes (Barrett et al. 2019). However, it appears that *Krameria* plastomes are exceptions to this trend. The ratios of substitution rates shown in figure 3 are consistent with trends reported in other lineages of photosynthetic plants: gene families with a photosynthetic function (*atp*, *ndh*, *pet*, *psa*, *psb*, *rbcL*, *ccsA*, *ycf3*, and *ycf4* in fig. 3) have lower *dN*/*dS* values, indicating stronger purifying selection, while housekeeping genes (*rpo*, *rpl*, and *rps*) and genes with other nonbioenergetic functions (*accD*, *clpP*, *ycf1*, and *ycf2*) tend to exhibit weaker degrees of purifying selection (Guisinger et al. 2010; Wicke et al. 2011; Li et al. 2013; Barnard-Kubow et al. 2014; Logacheva et al. 2016; Barrett et al. 2019).

Within this broad narrative, there are a few outliers (fig. 3). Alone among photosynthetic genes, *atpF* and *cemA* exhibit ω values that exceed 0.5, *atpF* with 42 variable sites of 555 (7.6%) and an average ω value of 0.80 and *cemA* with 76 variable sites of 690 (11.0%) and an average ω value of 0.52. The *atpF* gene is one of three *atp* genes involved in encoding the F_0 domain of the plastid ATP synthase (Wicke et al. 2011), which is involved in proton translocation across the thylakoid membrane but is interestingly the most commonly lost *atp* gene from the plastid genome (Mohanta et al. 2020). The gene *cemA* encodes a protein localized in the inner envelope membrane that is thought to assist with CO_2 uptake (Wicke et al. 2011) but has been shown not to be essential for photosynthetic reactions (Rolland et al. 1997). Consequently, it has been lost repeatedly in heterotrophic and parasitic lineages (Wolfe et al. 1992; Wicke et al. 2013; Banerjee and Stefanović 2019; Do et al. 2020; Li et al. 2021*b*) as well as in some autotrophic plants (Do et al. 2020). Four ribosomal protein genes with a housekeeping function also exhibit unusually elevated ω values: *rpl2* (3.5% variable sites, average ω of 1.35), *rpl22* (10.6% variable sites, average ω of 0.93), *rps7* (1.1% variable sites, average ω of 1.80), and *rps15* (12.5% variable sites, average ω of 0.99). Although ribosomal protein genes are generally maintained in plastomes, some are often found under positive selection (Wicke et al. 2014; Li et al. 2021*a*; Zeb et al. 2022) or lost entirely (Ni et al. 2016) in photosynthetic plants and certainly in heterotrophic plants (Wicke

et al. 2013; Samigullin et al. 2016; Graham et al. 2017; Banerjee and Stefanović 2019).

On the other hand, the *ndh* family of genes, which are primarily responsible for mitigating the effects of photooxidative stress, all appear to remain under strong purifying selection in *Krameria* plastomes (fig. 3). This is unexpected given that *ndh* genes are usually the first family of genes to be lost after the transition from autotrophy to heterotrophy (Wicke et al. 2011; Barrett and Davis 2012; Graham et al. 2017) or even before. Several autotrophic orchids (Kim et al. 2015; Lin et al. 2017), carnivorous plants (Silva et al. 2016, 2018; Nevill et al. 2019), aquatic plants (Peredo et al. 2013; Folk et al. 2020), cacti (Sanderson et al. 2015; Köhler et al. 2020), and other lineages (Ruhlman et al. 2015; Sabater 2021) have been found to have lost some or all *ndh* genes as well. The persistence of *ndh* genes, along with the presence of almost all other photosynthetic plastome genes under apparent strong purifying selection, implies that photosynthesis still plays an important role in the biology of *Krameria* species, perhaps because it allows continued productivity after hosts go dormant in the summer (Simpson 1989).

The increase in plastid genome size in the genus can be attributed to the accumulation of sequence length in intergenic regions. Expanded noncoding regions also account for the differences in length between the longer *K. erecta* plastome and the shorter *K. lanceolata* and *K. bicolor* plastomes. Coding regions make up only 51% of the total plastome size of *K. erecta*, compared with 53% for the other two species (and 57% for the much smaller *T. terrestris*). Accretion of tandem repeats appears to completely explain the intrageneric differences in plastome length and for a large part the bloat relative to *T. terrestris* (fig. 4; results provided in full in table S1). *Krameria lanceolata* has the shortest of the three *Krameria* plastid genomes at 171.9 kb, 6 kb smaller than those of *K. erecta*, at 177.8 kb. This disparity appears to be associated with the difference in sequence length contributed by short- and medium-length tandem repeats: 12.9 kb for *K. lanceolata* and 20.2 kb for *K. erecta*, a difference of 7.2 kb. *Krameria bicolor*, with an intermediate plastome size of 172.6 kb, has a commensurately intermediate sequence length contribution because of tandem repeats: 14.4 kb, 5.8 kb less than that of *K. erecta*. *Krameria erecta* has a plastome 19.6 kb larger than that of *T. terrestris* (plastome size, 158.2 kb) and has accumulated 11.4 kb more in tandem repeat sequence length. As has been observed for other large plastomes, these repeat regions are AT rich (Massouh et al. 2016; Li et al. 2019) and have resulted in the depression of GC% values of *Krameria* plastomes (tables 1, S1).

Accumulation of tandem repeats has been associated before with drastically increased plastome size (Guo et al. 2021) and has been implicated in accelerated plastome evolution leading to greater intraspecific variation (Massouh et al. 2016; Li et al. 2019). In addition, high tandem repeat content has been found to have a strong positive correlation with extensive plastome rearrangements in *Medicago* (Wu et al. 2021). However, there are several large plastid genomes in the rosids whose increased sizes do not coincide with the sequence length contributed by tandem repeats (table S2). For example, the largest published rosid plastome, that of *Vitis romanetti* (Xu and Xu 2021), is 232,020 bp long but contains only 804 short tandem repeats and 75 medium-length tandem repeats, which, in total, contribute 11,374 bp in sequence length (table S2). Instead, the relatively massive size of the *V. romanetti* plastome is almost entirely due to an increase in the size of the inverted repeat region and, consequently, several genes that are usually single copy being present twice (Xu and Xu 2021). In *Krameria*, there is an elevated accretion of repeats (fig. 4; table S2), but no rearrangements are apparent, and we do not have sampling to explore intraspecific variations at this point. Some tandem repeats are common to all three *Krameria* plastomes but absent in the Zygophyllaceae outgroup species (e.g., the pentanucleotide AAAAG repeat followed by the nine-nucleotide AATAGATAT repeat downstream of *atpH* and upstream of *atpF* or the pentanucleotide AAAAG repeat followed by the hexanucleotide AATAGT repeat downstream of *rpoC2* and upstream of *rps2*), while many others appear to be tip specific. Further research of the plastid genomics of this genus is needed to encompass additional species and to investigate whether there is a phylogenetic signal in the accumulation of these repeats, as well as to sample multiple individuals/populations from those species to explore intraspecific variation.

Plastomes of other autotrophs in the Zygophyllales are shorter than those of both *Krameria* and *Tribulus*. Notably, that of *Larrea tridentata* is 135,988 bp in length, largely because the pseudogenization and truncation of the nonbioenergetic *ycf2* gene (Gonçalves et al. 2019) cause significantly smaller inverted repeat regions (19.4 kb vs. 25.8 kb). Plastid genomes of other rosids range from potentially absent altogether (*Rafflesia* [Molina et al. 2014] and *Sapria* [Cai et al. 2021] in Rafflesiaceae, Malpighiales, Fabidae) to the abovementioned 232,020-bp-long example in *V. romanetti* (Vitaceae, Vitales, Rosidae; Xu and Xu 2021). The average rosid plastome is between 155 and 165 kb long, but several longer examples can be found (table S2), including within the fabids (Wang et al. 2017; Zhang et al. 2020; Lee et al. 2021). Given that Krameriaceae and Zygophyllaceae are the only families in Zygophyllales (which is sister to the rest of Fabidae), it is difficult to determine whether the larger plastome in *Krameria* is ancestral or derived. Thus, the plastome lengths of *Krameria* appear to be unremarkable for a rosid genus.

When it comes to tandem repeat accumulation, *Krameria* shares similarities with closely related taxa as well. Table S2 lists the numbers of short- and medium-length tandem repeats (along with total sequence length contributions) for a selection of rosid species. *Krameria lanceolata* and *K. bicolor* have repeat numbers akin to those of some species of Fabales and Malpighiales, orders that are part of the group sister to Zygophyllales, and those of *K. erecta* are slightly further elevated. On the other hand, some groups in Rosidae show tandem repeat accumulations similar to those of *T. terrestris* and *L. tridentata* (table S2). The order Rosales, also part of the group sister to Zygophyllales, contains plastomes with lower numbers of tandem repeat regions, similar to Zygophyllaceae. Altogether, this makes it difficult to conclude which is the ancestral state—the many tandem repeats of *Krameria* or the fewer tandem repeats of *Tribulus* and *Larrea*.

To sum up, *Krameria* plastid genomes, in structure at least, seem quite unremarkable, especially in the context of its taxonomic position. However, this finding itself appears quite remarkable given that this is a genus of obligate parasites that cannot survive without their hosts (Simpson 1989) and given the reductions in size and sequence composition observed in all other lineages of parasitic angiosperms (fig. 1). In particular, the continued retention of all *ndh* genes serves to underline the

unique nature of *Krameria*. As far as is currently known, *Krameria* is the only lineage of parasitic plants to retain their full complement of *ndh* genes as open reading frames. Their plastomes also maintain every other gene that their autotrophic neighbors do, and in some instances, they are even more complete in terms of coding content (e.g., in comparison with *L. tridentata*).

Unlike those of every other parasitic plant lineage, *Krameria* plastomes do not appear to have been impacted by the genomic effects of the parasitic reduction syndrome (Colwell 1994). This may be because of the hot and arid environments in which they grow, where their hosts seasonally go dormant; hence, they often must continue to sustain themselves longer than other heterotrophs tend to have to (Simpson 1989). It is also probable that because *Krameria* species establish haustorial connections solely for the acquisition of water and dissolved nutrients (Brokamp et al. 2012), they therefore still require the full complement of photosynthetic genes in order to produce their own photosynthates. Despite its low extant species diversity, *Krameria* is thought to represent a relatively old lineage (stem age of 34–90 Myr; Magallón et al. 2015), and therefore it cannot be concluded that plastomes in this group are unaffected simply because they are in an "early" stage of reduction. Our results thus suggest that *Krameria* plastomes are evolutionarily stable and continue to be central to the functioning and survival of these plants.

Acknowledgments

This work was supported by the Natural Sciences and Engineering Research Council of Canada (grant 326439), the Canada Foundation for Innovation (grant 12810), and Ontario Research Funds. We thank Craig Barrett and one anonymous reviewer for their constructive feedback. Open access publishing funded by Hendrix College.

Literature Cited

Altschul SF, W Gish, W Miller, EW Myers, DJ Lipman 1990 Basic local alignment search tool. J Mol Biol 215:403–410

Angiosperm Phylogeny Group, MW Chase, MJM Christenhusz, MF Fay, JW Byng, WS Judd, DE Soltis, et al 2016 An update of the Angiosperm Phylogeny Group classification for the orders and families of flowering plants: APG IV. Bot J Linn Soc 181:1–20.

Banerjee A, S Stefanović 2019 Caught in action: fine-scale plastome evolution in the parasitic plants of *Cuscuta* section *Ceratophorae* (Convolvulaceae). Plant Mol Biol 100:621–634.

——— 2020 Reconstructing plastome evolution across the phylogenetic backbone of the parasitic plant genus *Cuscuta* (Convolvulaceae). Bot J Linn Soc 194:423–438.

Barnard-Kubow KB, DB Sloan, LF Galloway 2014 Correlation between sequence divergence and polymorphism reveals similar evolutionary mechanisms acting across multiple timescales in a rapidly evolving plastid genome. BMC Evol Biol 14:268.

Barrett CF, JI Davis 2012 The plastid genome of the mycoheterotrophic *Corallorhiza striata* (Orchidaceae) is in the relatively early stages of degradation. Am J Bot 99:1513–1523.

Barrett CF, JV Freudenstein, J Li, DR Mayfield-Jones, L Perez, JC Pires, C Santos 2014 Investigating the path of plastid genome degradation in an early-transitional clade of heterotrophic orchids, and implications for heterotrophic angiosperms. Mol Biol Evol 31:3095–3112.

Barrett CF, BT Sinn, AH Kennedy 2019 Unprecedented parallel photosynthetic losses in a heterotrophic orchid genus. Mol Biol Evol 36:1884–1901.

Bellot S, N Cusimano, S Luo, G Sun, S Zarre, A Gröger, E Temsch, SS Renner 2016 Assembled plastid and mitochondrial genomes, as well as nuclear genes, place the parasite family Cynomoriaceae in the Saxifragales. Genome Biol Evol 8:2214–2230.

Bellot S, SS Renner 2015 The plastomes of two species in the endoparasite genus *Pilostyles* (Apodanthaceae) each retain just five or six possibly functional genes. Genome Biol Evol 8:189–201.

Bodenhofer U, E Bonatesta, C Horejš-Kainrath, S Hochreiter 2015 msa: an R package for multiple sequence alignment. Bioinformatics 31:3997–3999.

Brokamp G, N Dostert, F Cáceres-H, M Weigend 2012 Parasitism and haustorium anatomy of *Krameria lappacea* (Dombey) Burdet & B.B. Simpson (Krameriaceae), an endangered medicinal plant from the Andean deserts. J Arid Environ 83:94–100.

Cai L, BJ Arnold, Z Xi, DE Khost, N Patel, CB Hartmann, S Manickam 2021 Deeply altered genome architecture in the endoparasitic flowering plant *Sapria himalayana* Griff. (Rafflesiaceae). Curr Biol 31:1002–1011.

Catalogue of Life Partnership 2017 APG IV: Angiosperm Phylogeny Group classification for the orders and families of flowering plants. https://doi.org/10.15468/fzuaam.

Chen X, D Fang, C Wu, B Liu, Y Liu, SK Sahu, B Song 2020 Comparative plastome analysis of root- and stem-feeding parasites of Santalales untangle the footprints of feeding mode and lifestyle transitions. Genome Biol Evol 12:3663–3676.

Colwell AE 1994 Genome evolution in a non-photosynthetic plant, *Conopholis americana*. PhD diss. Washington University, St Louis.

Cronquist A 1981 An integrated system of classification of flowering plants. Columbia University Press, New York.

Darling AE, B Mau, NT Perna 2010 progressiveMauve: multiple genome alignment with gene gain, loss and rearrangement. PLoS ONE 5:e11147.

Do HDK, C Kim, MW Chase, JH Kim 2020 Implications of plastome evolution in the true lilies (monocot order Liliales). Mol Phylogenet Evol 148:106818.

Doyle JJ, JL Doyle 1987 A rapid DNA isolation procedure for small quantities of fresh leaf tissue. Phytochem Bull 19:11–15.

Folk RA, N Sewnath, C-L Xiang, BT Sinn, RP Guralnick 2020 Degradation of key photosynthetic genes in the critically endangered semi-aquatic flowering plant *Saniculiphyllum guangxiense* (Saxifragaceae). BMC Plant Biol 20:324.

Gonçalves DJP, BB Simpson, EM Ortiz, GH Shimizu, RK Jansen 2019 Incongruence between gene trees and species trees and phylogenetic signal variation in plastid genes. Mol Phylogenet Evol 138:219–232.

Graham SW, VK Lam, VS Merckx 2017 Plastomes on the edge: the evolutionary breakdown of mycoheterotroph plastid genomes. New Phytol 214:48–55.

Greiner S, P Lehwark, R Bock 2019 OrganellarGenomeDRAW (OGDRAW) version 1.3.1: expanded toolkit for the graphical visualization of organellar genomes. Nucleic Acids Res 47:W59–W64.

Guisinger MM, TW Chumley, JV Kuehl, JL Boore, RK Jansen 2010 Implications of the plastid genome sequence of *Typha* (Typhaceae, Poales) for understanding genome evolution in Poaceae. J Mol Evol 70:149–166.

Guo YY, JX Yang, HK Li, HS Zhao 2021 Chloroplast genomes of two species of Cypripedium: expanded genome size and proliferation of AT-biased repeat sequences. Front Plant Sci 12:609729.

Hausner G, R Olson, D Simon, I Johnson, ER Sanders, KG Karol, RM McCourt, S Zimmerly 2006 Origin and evolution of the chloroplast *trnK* (*matK*) intron: a model for evolution of group II intron RNA structures. Mol Biol Evol 23:380–391.

Heide-Jorgensen H 2008 Parasitic flowering plants. Brill, Leiden.

Jacquemyn H, V Merckx 2019 Mycorrhizal symbioses and the evolution of trophic modes in plants. J Ecol 107:1567–1581.

Jin JJ, WB Yu, JB Yang, Y Song, CW de Pamphilis, T-S Li, D-Z Li 2020 GetOrganelle: a fast and versatile toolkit for accurate de novo assembly of organelle genomes. Genome Biol 21:241.

Joshi NA, JN Fass 2011 Sickle: a sliding-window, adaptive, quality-based trimming tool for FastQ files. https://github.com/najoshi/sickle.

Jost M, J Naumann, N Rocamundi, AA Cocucci, S Wanke 2020 The first plastid genome of the holoparasitic genus *Prosopanche* (Hydnoraceae). Plants 9:306.

Kim HT, JS Kim, MJ Moore, KM Neubig, NH Williams, WM Whitten, J-H Kim 2015 Seven new complete plastome sequences reveal rampant independent loss of the *ndh* gene family across orchids and associated instability of the inverted repeat/small single-copy region boundaries. PLoS ONE 10:e0142215.

Köhler M, M Reginato, TT Souza-Chies, LC Majure 2020 Insights Into chloroplast genome evolution across Opuntioideae (Cactaceae) reveals robust yet sometimes conflicting phylogenetic topologies. Front Plant Sci 11:729.

Kwon E-C, J-H Kim, N-S Kim 2020 Comprehensive genomic analyses with 115 plastomes from algae to seed plants: structure, gene contents, GC contents, and introns. Genes Genomics 42:553–570.

Lee C, IS Choi, D Cardoso, HC de Lima, LP de Queiroz, MF Wojciechowski, RK Jansen, TA Ruhlman 2021 The chicken or the egg? plastome evolution and an independent loss of the inverted repeat in papilionoid legumes. Plant J 107:861–875.

Li X, Y Li, SP Sylvester, M Zang, YA El-Kassaby, Y Fang 2021*a* Evolutionary patterns of nucleotide substitution rates in plastid genomes of *Quercus*. Ecol Evol 11:13401–13414.

Li X, J-B Yang, H Wang, Y Song, RT Corlett, X Yao, D-Z Li, W-B Yu 2021*b* Plastid NDH pseudogenization and gene loss in a recently derived lineage from the largest hemiparasitic plant genus *Pedicularis* (Orobanchaceae). Plant Cell Physiol 62:971–984.

Li X, TC Zhang, Q Qiao, Z Ren, J Zhao, T Yonezawa, M Hasegawa, MJC Crabbe, J Li, Y Zhong 2013 Complete chloroplast genome sequence of holoparasite *Cistanche deserticola* (Orobanchaceae) reveals gene loss and horizontal gene transfer from its host *Haloxylon ammodendron* (Chenopodiaceae). PLoS ONE 8:e58747.

Li Y, J-G Zhou, X-L Chen, Y-X Cui, Z-C Xu, Y-H Li, J-Y Song, B-Z Duan, H Yao 2017 Gene losses and partial deletion of small single-copy regions of the chloroplast genomes of two hemiparasitic *Taxillus* species. Sci Rep 7:12834.

Li Z-H, X Ma, D-Y Wang, Y-X Li, C-W Wang, X-H Jin 2019 Evolution of plastid genomes of *Holcoglossum* (Orchidaceae) with recent radiation. BMC Evol Biol 19:63.

Lin CS, JJW Chen, CC Chiu, HCW Hsiao, C-J Yang, X-H Jin, J Leebens-Mack, et al 2017 Concomitant loss of NDH complex-related genes within chloroplast and nuclear genomes in some orchids. Plant J 90:994–1006.

Liu Z-F, H Ma, X-Q Ci, L Li, Y Song, B Liu, H-W Li, et al 2021 Can plastid genome sequencing be used for species identification in Lauraceae? Bot J Linn Soc 197:1–14.

Logacheva MD, MI Schelkunov, VY Shtratnikova, MV Matveeva, AA Penin 2016 Comparative analysis of plastid genomes of non-photosynthetic Ericaceae and their photosynthetic relatives. Sci Rep 6:30042.

Lowe TM, PP Chan 2016 tRNAscan-SE on-line: integrating search and context for analysis of transfer RNA genes. Nucleic Acids Res 44:W54–W57.

Madeira F, YM Park, J Lee, N Buso, T Gur, N Madhusoodanan, P Basutkar, et al 2019 The EMBL-EBI search and sequence analysis tools APIs in 2019. Nucleic Acids Res 47:W636–W641.

Magallón S, S Gómez-Acevedo, LL Sánchez-Reyes, T Hernández-Hernández 2015 A metacalibrated time-tree documents the early rise of flowering plant phylogenetic diversity. New Phytol 207:437–453.

Massouh A, J Schubert, L Yaneva-Roder, ES Ulbricht-Jones, A Zupok, MTJ Johnson, SI Wright, et al 2016 Spontaneous chloroplast mutants mostly occur by replication slippage and show a biased pattern in the plastome of *Oenothera*. Plant Cell 28:911–929.

McNeal JR, JV Kuehl, JL Boore, CW de Pamphilis 2007 Complete plastid genome sequences suggest strong selection for retention of photosynthetic genes in the parasitic plant genus *Cuscuta*. BMC Plant Biol 7:57.

Merckx V 2013 Mycoheterotrophy: the biology of plants living on fungi. Springer, New York.

Mohanta TK, AK Mishra, A Khan, A Hashem, EF Abd Allah, A Al-Harrasi 2020 Gene loss and evolution of the plastome. Genes 11:1133.

Molina J, KM Hazzouri, D Nickrent, M Geisler, RS Meyer, MM Pentony, JM Flowers, et al 2014 Possible loss of the chloroplast genome in the parasitic flowering plant *Rafflesia lagascae* (Rafflesiaceae). Mol Biol Evol 31:793–803.

Naumann J, JP Der, EK Wafula, SS Jones, ST Wagner, LA Honaas, PE Ralph, et al 2016 Detecting and characterizing the highly divergent plastid genome of the nonphotosynthetic parasitic plant *Hydnora visseri* (Hydnoraceae). Genome Biol Evol 8:345–363.

Nevill PG, KA Howell, AT Cross, AV Williams, X Zhong, J Tonti-Filippini, LM Boykin, KW Dixon, I Small 2019 Plastome-wide rearrangements and gene losses in carnivorous Droseraceae. Genome Biol Evol 11:472–485.

Ni L, Z Zhao, H Xu, S Chen, G Dorje 2016 The complete chloroplast genome of *Gentiana straminea* (Gentianaceae), an endemic species to the Sino-Himalayan subregion. Gene 577:281–288.

Nickrent D 2020 Parasitic angiosperms: how often and how many? Taxon 69:5–27.

Paradis E, J Claude, K Strimmer 2004 APE: analyses of phylogenetics and evolution in R language. Bioinformatics 20:289–290.

Peredo EL, UM King, DH Les 2013 The plastid genome of *Najas flexilis*: adaptation to submersed environments is accompanied by the complete loss of the NDH complex in an aquatic angiosperm. PloS ONE 8:1.

Pereira JBS, AM Giulietti, ES Pires, M Laux, MTC Watanabe, RRM Oliveira, S Vasconcelos, G Oliveira 2021 Chloroplast genomes of key species shed light on the evolution of the ancient genus *Isoetes*. J Syst Evol 59:429–441.

Popescu AA, KT Huber, E Paradis 2012 ape 3.0: new tools for distance-based phylogenetics and evolutionary analysis in R. Bioinformatics 28:1536–1537.

R Core Team 2000 R: a language and environment for statistical computing. R Foundation for Statistical Computing, Vienna. https://www.R-project.org/.

Rolland N, AJ Dorne, G Amoroso, DF Sültemeyer, J Joyard, JD Rochaix 1997 Disruption of the plastid *ycf10* open reading frame affects uptake of inorganic carbon in the chloroplast of *Chlamydomonas*. Embo J 16:6713–6726.

Roquet C, É Coissac, C Cruaud, M Boleda, F Boyer, A Alberti, L Gielly, et al 2016 Understanding the evolution of holoparasitic plants: the complete plastid genome of the holoparasite *Cytinus hypocistis* (Cytinaceae). Ann Bot 118:885–896.

Ruhlman T, W-J Chang, JJW Chen, Y-T Huang, M-T Chan, J Zhang, D-C Liao, et al 2015 NDH expression marks major transitions in

plant evolution and reveals coordinate intracellular gene loss. BMC Plant Biol 15:100.

Sabater B 2021 On the edge of dispensability, the chloroplast *ndh* genes. Int J Mol Sci 22:12505.

Samigullin TH, MD Logacheva, AA Penin, CM Vallejo-Roman 2016 Complete plastid genome of the recent holoparasite *Lathraea squamaria* reveals earliest stages of plastome reduction in Orobanchaceae. PLoS ONE 11:e0150718.

Sanderson MJ, D Copetti, A Búrquez, E Bustamante, JLM Charboneau, LE Eguiarte, S Kumar, et al 2015 Exceptional reduction of the plastid genome of saguaro cactus (*Carnegiea gigantea*): loss of the *ndh* gene suite and inverted repeat. Am J Bot 102:1115–1127.

Schneider AC, T Braukmann, A Banerjee, S Stefanovic 2018 Convergent plastome evolution and gene loss in holoparasitic Lennoaceae. Genome Biol Evol 10:2663–2670.

Sheahan MC, MW Chase 1996 A phylogenetic analysis of Zygophyllaceae R.Br. based on morphological, anatomical and *rbc*L DNA sequence data. Bot J Linn Soc 122:279–300.

Shin HW, NS Lee 2018 Understanding plastome evolution in hemiparasitic Santalales: complete chloroplast genomes of three species, *Dendrotrophe varians*, *Helixanthera parasitica*, and *Macrosolen cochinchinensis*. PLoS ONE 13:e0200293.

Silva SR, YCA Diaz, HA Penha, DG Pinheiro, CC Fernandes, VFO Miranda, TP Michael, AM Varani 2016 The chloroplast genome of *Utricularia reniformis* sheds light on the evolution of the *ndh* gene complex of terrestrial carnivorous plants from the Lentibulariaceae family. PLoS ONE 11:e0165176.

Silva SR, TP Michael, EJ Meer, DG Pinheiro, AM Varani, VFO Miranda 2018 Comparative genomic analysis of *Genlisea* (corkscrew plants—Lentibulariaceae) chloroplast genomes reveals an increasing loss of the *ndh* genes. PLoS ONE 13:e0190321.

Simpson BB 1989 Krameriaceae. Flora Neotrop 49:1–108.

Simpson BB, A Weeks, DM Helfgott, LL Larkin 2004 Species relationships in *Krameria* (Krameriaceae) based on ITS sequences and morphology: implications for character utility and biogeography. Syst Bot 29:97–108.

Soltis DE, PS Soltis, MW Chase, ME Mort, DC Albach, M Zanis, V Savolainen, et al 2000 Angiosperm phylogeny inferred from 18S rDNA, *rbcL*, and *atpB* sequences. Bot J Linn Soc 133:381–461.

Su H-J, TJ Barkman, W Hao, SS Jones, J Naumann, E Skippington, EK Wafula, J-M Hu, JD Palmer, CW de Pamphilis 2019 Novel genetic code and record-setting AT-richness in the highly reduced plastid genome of the holoparasitic plant *Balanophora*. Proc Natl Acad Sci USA 116:934–943.

Wang H, MJ Moore, PS Soltis, CD Bell, SF Brockington, R Alexandre, CC Davis, M Latvis, SR Manchester, DE Soltis 2009 Rosid radiation and the rapid rise of angiosperm-dominated forests. Proc Natl Acad Sci USA 106:3853–3858.

Wang Y-H, X-J Qu, S-Y Chen, D-Z Li, T-S Yi 2017 Plastomes of Mimosoideae: structural and size variation, sequence divergence, and phylogenetic implication. Tree Genet Genomes 13:41.

Wicke S, KF Müller, CW de Pamphilis, D Quandt, S Bellot, GM Schneeweiss 2016 Mechanistic model of evolutionary rate variation en route to a nonphotosynthetic lifestyle in plants. Proc Natl Acad Sci USA 113:9045–9050.

Wicke S, KF Müller, CW de Pamphilis, D Quandt, NJ Wickett, Y Zhang, SS Renner, GM Schneeweiss 2013 Mechanisms of functional and physical genome reduction in photosynthetic and nonphotosynthetic parasitic plants of the Broomrape family. Plant Cell 25:3711–3725.

Wicke S, J Naumann 2018 Molecular evolution of plastid genomes in parasitic flowering plants. Adv Bot Res 85:315–347.

Wicke S, B Schäferhoff, CW de Pamphilis, KF Müller 2014 Disproportional plastome-wide increase of substitution rates and relaxed purifying selection in genes of carnivorous Lentibulariaceae. Mol Biol Evol 31:529–545.

Wicke S, GM Schneeweiss, CW de Pamphilis, KF Muller, D Quandt 2011 The evolution of the plastid chromosome in land plants: gene content, gene order, gene function. Plant Mol Biol 76:273–297.

Wolfe KH, CW Morden, SC Ems, JD Palmer 1992 Rapid evolution of the plastid translational apparatus in a nonphotosynthetic plant: loss or accelerated sequence evolution of tRNA and ribosomal protein genes. J Mol Evol 35:304–317.

Wu CS, TJ Wang, CW Wu, YN Wang, SM Chaw 2017 Plastome evolution in the sole hemiparasitic genus laurel dodder (*Cassytha*) and insights into the plastid phylogenomics of Lauraceae. Genome Biol Evol 9:2604–2614.

Wu S, J Chen, Y Li, A Liu, A Li, M Yin, N Shrestha, J Liu, G Ren 2021 Extensive genomic rearrangements mediated by repetitive sequences in plastomes of *Medicago* and its relatives. BMC Plant Biol 21:421.

Xu G, W Xu 2021 Complete chloroplast genomes of Chinese wildgrowing *Vitis* species: molecular structures and comparative and adaptive radiation analysis. Protoplasma 258:559–571.

Yan J, N Zhang, Y Duan 2019 The complete chloroplast genome sequence of *Tribulus terrestris*, an important traditional Chinese medicine. Mitochondrial DNA B Resour 4:3108–3109.

Yang Y, S-L He 2019 The complete chloroplast genome of *Malania oleifera* (Olacaceae), an endangered species in China. Mitochondrial DNA B Resour 4:1867–1868.

Zeb U, X Wang, A AzizUllah, S Fiaz, H Khan, S Ullah, H Ali, K Shahzad 2022 Comparative genome sequence and phylogenetic analysis of chloroplast for evolutionary relationship among *Pinus* species. Saudi J Biol Sci 29:1618–1627.

Zhang R, Y-H Wang, J-J Jin, GW Stull, A Bruneau, D Cardoso, L Paganucci De Queiroz, et al 2020 Exploration of plastid phylogenomic conflict yields new insights into the deep relationships of Leguminosae. Syst Biol 69:613–622.